

# Lifshitz transitions and zero point lattice fluctuations in sulfur hydride showing near room temperature superconductivity

Antonio Bianconi<sup>1,2,3</sup> and Thomas Jarlborg<sup>4</sup>

<sup>1</sup> *RICMASS, Rome International Center for Materials Science, Superstripes, Via dei Sabelli 119A, 00185 Rome, Italy*

<sup>2</sup> *Institute of Crystallography, Consiglio Nazionale delle Ricerche, via Salaria, 00015 Monterotondo, Italy*

<sup>3</sup> *INSTM, Consorzio Interuniversitario Nazionale per la Scienza e Tecnologia dei Materiali, Rome Udr, Italy*

<sup>4</sup> *DPMC, University of Geneva, 24 Quai Ernest-Ansermet, CH-1211 Geneva 4, Switzerland*

The presence of possible electronic topological transitions for the appearing of new Fermi surface spots in sulfur hydride H<sub>3</sub>S metal induced by increasing pressure above 100 GPa has been studied by band structure calculations. Here we report the presence of two topological Lifshitz transitions at two critical pressures  $P_{c1} = 110$  GPa, and  $P_{c2} = 180$  GPa. At the first Lifshitz transition, around  $P_{c1} = 110$  GPa, three new Fermi surface spots appear due to the tops of three hole-like bands  $\beta$ ,  $\gamma_1$ , and  $\gamma_2$  pushed up by pressure which cross the chemical potential at the  $\Gamma$  point of the Brillouin zone. These anisotropic bands are characterized by a flat dispersion in the  $\Gamma - M$  direction and a steep dispersion in the  $\Gamma - X$  direction. The second Lifshitz transition at  $P_{c2} = 180$  GPa is due to the appearing of a new Fermi surface spot between the  $\Gamma$  and M direction of the Brillouin zone which is due to band edge of the  $\delta$  band pushed above the chemical potential by the high pressure. The amplitude of the energy fluctuations of the band edges due to atomic zero point motion has been calculated. The large calculated zero point motion of the hydrogen atoms induce energy fluctuations of the order of hundreds meV of the band edges and therefore of the Lifshitz transitions. We have focused on the fine details of the electronic structure in the pressure range from 170 GPa to 250 GPa where Emerets's experiments show that the critical temperature of H<sub>3</sub>S goes from  $T_c = 203$  K to  $T_c = 180$  K and the isotope coefficient shows non negligible variations between 0.25 and 0.5. The present results show that in this pressure range the condensates in the 4 small hole pockets formed by the  $\beta$ ,  $\gamma_1$ ,  $\gamma_2$  and  $\delta$  bands are beyond Migdal approximation because including dynamical zero point fluctuations  $\omega_0/E_F \sim 1$ . In particular the appearing of the hole-like  $\delta$  Fermi surface is associated with the sharp quasi-1D peak in the DOS pushed above the chemical potential by pressure. Since the superconducting phase of H<sub>3</sub>S is expected to be in the clean limit with coexisting condensates in the different Fermi surfaces, our results show that the condensates in the  $\beta$ ,  $\gamma_1$ ,  $\gamma_2$  and  $\delta$  Fermi surface pockets should be in the BEC-BCS crossover regime coexisting with other condensates in the BCS regime in the large Fermi surfaces.

PACS numbers: 74.20.Pq, 74.72.-h, 74.25.Jb

## I. INTRODUCTION.

Following early claims of 190 K superconductivity in sulfur hydrides at very high pressure [1], new results of near room temperature superconductivity with  $T_c=203$  K i.e., at only -70 °C [2] have been presented on June 17, 2015 at Superstripes 2015 conference in Ischia, Italy [3] and they have triggered a very high scientific interest [4]. The recent work of Emerets's group [2] shows the Meissner effect and the pressure dependent critical temperature of H<sub>3</sub>S and D<sub>3</sub>S. The experimental discovery of near room temperature superconductivity in sulfur hydride H<sub>2</sub>S at very high pressure was predicted by [5] to occur in high pressure metallic H<sub>3</sub>S phase with  $Im\bar{3}m$  lattice symmetry with two formula units in each unit cell 2(H<sub>3</sub>S), resulting from 2(H<sub>2</sub>S) + H<sub>2</sub> disproportion at very high pressure. The theoretical predictions of Duan et al. [5] using the evolutionary algorithm Universal Structure Predictor: Evolutionary Xtallography (USPEX) [6] have been confirmed by several theoretical works [7–9].

These results have triggered today the materials research for room temperature superconductors in different hydrides at extreme high pressures [30–34]. While

conventional phonon mediated pairing is well accepted to be in action. the critical temperature cannot be explained by the standard weak coupling BCS model for a single band metal. There is agreement that the near room temperature superconductivity in these systems [10–15] is an extreme case of the non standard BCS regime predicted for metallic hydrogen and hydrides [16–24] showing high energy phonons, due to low Z elements, strong coupling, and anomalous or negative dielectric constant. This scenario should result from a complex balance of many different parameters controlling the critical temperature. In fact in the single band approximation  $T_c$  increases with both phonon energy and coupling strength for the standard BCS scenario in weak coupling regime, but for extreme strong electron-phonon coupling the critical temperature decreases since the phonon energy is pushed toward zero, the lattice structure collapses and the system is in the verge of a catastrophe. Therefore it is known that materials research for room temperate superconductivity cannot be driven simply by looking to increase the phonon energy and coupling strength in the cooper pairing. Advances in this field requires the development of the physics for the optimization of the ampli-

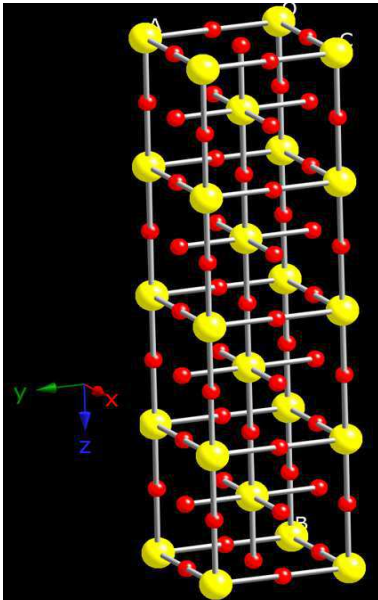


FIG. 1: (Color online) The crystalline structure of  $\text{H}_3\text{S}$  with  $Im\bar{3}m$  lattice symmetry, with two formula units per unit cell, with sulfur (yellow large spheres) and hydrogen atoms (red small spheres). The linear S-H-S hydrogen bonds along the a, b and c axis in the  $Im\bar{3}m$  lattice of  $\text{H}_3\text{S}$ , form a first 3D network of three linear chains of covalent bonds crossing at the sulfur atom at  $S1(0,0,0)$ , which coexists with a second 3D network of other three linear chains of covalent bonds (solid black lines) crossing at the sulfur atom at  $S1(0.5,0.5,0.5)$ .

fication of the critical temperature in the frame of non standard BCS theories. In non standard BCS theories the critical temperature is controlled also by other key factors as (i) the negative dielectric constant [17, 19, 23], controlling the electron-electron interaction and (ii) the shape resonance in superconducting gaps, [25–27] controlling the many body configuration interaction between pairs driving the formation of the superfluid condensate, like the Feshbach resonances in ultracold atoms. Several details of the normal phase could become key ingredients: a) the complex Fermiology, beyond the single band model; b) percolation phenomena in complex inhomogeneous systems with nanoscale phase separation, beyond the usually assumed homogeneous lattice [28, 29]; c) the anomalous electron-phonon interactions, beyond usually assumed Migdal approximation; d) the strong electronic correlations in the electron fluid near a band edge with very low Fermi energy, beyond the usually assumed Fermi gas approximation; e) the anomalous or negative dielectric response controlling the electron-electron interaction; and in the superconducting phase not only pair formation but also exchange-like terms between pairs controlling the condensation energy and phase coherence become unavoidable terms for the formation and stability of high temperature superconducting condensates with short coherence lengths. The overall features of superconductivity in  $\text{H}_3\text{S}$  show that it is in a non standard BCS

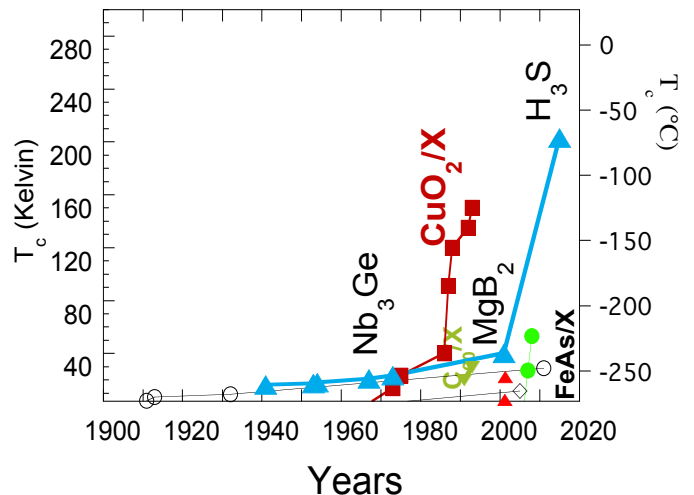


FIG. 2: (Color online) The superconducting critical temperature of superconducting elements, open black circles, binary intermetallics, filled blue triangles, and ternary and quaternary oxide layered perovskites made of  $\text{CuO}_2$  atomic layers with different X spacer layers (filled red squares) coefficient as a function of the year of the discovery

regime like other binary intermetallics, as A15 systems, diborides and hydrides. A15 compounds (like  $\text{Nb}_3\text{Ge}$ ) have the same  $Im\bar{3}m$  lattice structure [35] as  $\text{H}_3\text{S}$  above 100 GPa (shown in Fig.1) which is made of two three dimensional networks of atomic wires as noticed by Friedel [36] and superconductivity appear in highly inhomogeneous phases at the edge of a lattice catastrophe due incipient structural phase transitions [37–39] giving complex pattern of defects and local lattice fluctuations [40–42]. Moreover there is agreement [10–14] that the superconductivity phase in  $\text{H}_3\text{S}$  is in the clean limit requiring a non standard anisotropic BCS theory. In fact the standard BCS assumes a single effective band (resulting from the dirty limit), a single gap and a single coherence length with the critical temperature given by standard McMillan or Eliashberg formula. In the clean limit non standard BCS theories are required, as discussed in the Appendix, where the multiple gaps in different spots of the k-space are connected each other by a complex self consistent formula and the condensation of a quantum coherent macroscopic superconducting phase is generated by multiple condensates with different gaps and different coherence lengths. Therefore the superconducting phase in  $\text{H}_3\text{S}$  is similar to doped magnesium diboride, which has been called the "hydrogen atom" multigap superconductivity in the clean limit.

The discovery of superconductivity in  $\text{MgB}_2$  in 2001 has falsified the common theoretical assumption used by standard BCS approximation since 1957, that anisotropic pairing in the clean limit was not possible in normal de-

fective materials. The standard BCS theory, considering a single band and single gap, failed to predict accurately the unusually high transition temperature, the effects of isotope substitution on the critical transition temperature, and the anomalous specific heat of  $\text{MgB}_2$ . While some authors proposed the multiband superconductivity theory [43] in the clean limit and weak coupling, it was rapidly shown the need of strong coupling anisotropic two band Eliashberg theory to describe this unexpected novel superconducting phase [44, 45]. However it was rapidly shown that the isostructural  $\text{AlB}_2$  system with only  $\pi$  electrons at the Fermi level becomes superconductor only when the chemical doping pushes the top of the  $\sigma$  band above the chemical potential forming two small hole-like  $\sigma$  Fermi pockets [46]. Moreover because of zero point atomic fluctuations, [47] and lattice fluctuations in presence of phonon softening and phase separation [48, 49] the Fermi energy in the  $\sigma$  band is time and space dependent therefore the Migdal approximation  $\omega_0/E_F < 1$  is violated and the Eliashberg theory fails tuning the chemical potential over a range of 600 meV. Therefore in spite of the conventional phonon mediated pairing, the 40 K superconducting phase in magnesium diboride need a non standard BCS theory. Considering all data collected in diborides doped with Sc and Al for Mg or with C for B it was possible to collect the variation of the two superconducting gaps and the critical temperature as a function of the energy separation between the top of the  $\sigma$  band and the chemical potential[50]. The superconducting  $\sigma$  gaps are much larger than the gaps in the large  $\pi$  Fermi surfaces and evolve as a function of the energy separation of the top of the  $\sigma$  band and the the chemical potential [50]. In spite the percentage of the partial electronic density of states,  $\text{DOS}(\sigma)$ , relative to the total  $\text{DOS}(tot)$  usually entering in the standard McMillan formula for  $T_c$ , the large superconducting  $\sigma$  gap drives the system to the highest critical temperature known in binary intermetallics before the recent discovery of Eremets's group [2]. In a single band metal, where  $\omega_0/E_F \sim 1$  the Migdal and in the adiabatic approximations [52] fail, the system enters in the BEC-BCS crossover [51, 53] and both weak coupling BCS[54] and strong coupling Eliashberg theories breakdown. On the contrary in a system with multiple condensates only one or two of the Fermi surface spots are in the BEC-BCS crossover, while other condensates in the large Fermi surfaces are in the BCS regime, it has been shown that the problem can be described using the correct multigap anisotropic BCS theory(MABCS)[50, 55] including Bogolyubov [56], Gorkov[57], Blatt[59] contributions and the condensation energy[60, 61] related with Josephson-like[58] terms (see Appendix). The condensation energy[60] is relevant a) in the BEC-BCS crossover  $\Delta_n/E_{F_n} \sim 1$  and in the formation of the superconducting quantum coherent phase with a single  $T_c$  in a system made of multiple gaps  $\Delta_n$  in different bands with different Fermi energies  $E_{F_n}$ . Here the chemical potential going from the normal to the superconducting phase below  $T_c$ , which on the contrary is considered to be negligible

in the standard BCS regime become relevant. In these cases it is necessary to include the many body condensation energy in the calculation of the superconducting gap. The condensation energy of the pairs is determined by many body configuration interaction between pairs forming the single macroscopic superconducting quantum coherent phase. The results of the correct MABCS theory [50] show that superconducting magnesium diboride is in a regime of multi-condensates where one condensate in the  $\sigma$  band is in the BEC-BCS crossover while other  $\pi$  bands are in the BCS regime with a small but finite pair Josephson-like exchange term.

## II. LIFSHITZ TRANSITIONS.

Here the new physics is the fine energy tuning of the chemical potential across selected band edges in a multi-band system. The topological changes of the Fermi surface of the normal phase caused by external pressure, chemical pressure, misfit strain, chemical substitution, variation of the electronic density changing the chemical potential, are called Lifshitz transitions [62]. In many cases Lifshitz transitions appear on points or lines of high symmetry in the Brillouin zone and are associated with changes of the symmetry or dimensionality of the wave functions of the electrons at the Fermi level in critical Fermi surfaces. The Lifshitz transitions are revealed experimentally by anomalies in lattice parameters, in the density of states near the Fermi energy, in elastic properties, in anomalous thermodynamic and transport properties of metallic materials [63]. Lifshitz [1] noted that at zero temperature,  $T = 0$ , Lifshitz transitions are true phase transitions of order 2.5 (as in Ehrenfest's classification) therefore are called "2.5 Lifshitz transition". A sharp Lifshitz transition at  $T=0$ , at high temperature shows a crossover character and in presence of strong interactions the 2.5 phase transition becomes first order with a phase separation between two phases where the chemical potential in each phase is shifted above and below the Lifshitz transition respectively[49, 64, 65] driving the system well tuned at a Lifshitz transition on the verge of a lattice catastrophe as shown in the case of  $\text{A15}$  and diborides. While in the early times the interest was focused on Lifshitz transitions in single band metals but now the interest is addressed to Lifshitz transitions in multi-band metals. Multi-band metals with different Fermi surfaces show multi-gap superconductivity. The case of interest for achievement of the optimization of high critical temperature is to reach particular Lifshitz transitions where a small number of electrons in a new appearing Fermi surface spot are in the extreme strong coupling regime in the antiadiabatic  $\omega_0/E_{F_n} \sim 1$  and BEC-BCS crossover  $\Delta_n/E_{F_n} \sim 1$  [66].without the lattice catastrophe since the majority of the electron gas is in large Fermi surfaces well in the Migdal approximation  $\omega_0/E_{F_n} < 1$ , in fact in this regime the shape resonances in the superconducting gaps can be ptimized to amplify

the critical temperature to the highest value. The theory of the shape resonance in superconducting gaps, active in the proximity of Lifshitz transitions in presence of a large zero point lattice motion, has been proposed for cuprates [25–27, 67–70] has been tested in diborides [46, 50] and confirmed in iron based superconductors [71–77]. The shape resonance theory, considers the relevant contribution of the exchange interaction between pairs for further rise of the critical temperature. Moreover the coupling constant for pairing is renormalized i.e., it should be corrected by a coefficient "F" given by the quantum overlap between superconducting pairs. The shape resonance in superconducting gaps is a Josephson-like term describing a contact interaction between pairs which increases the critical temperature for the pairs condensation, very similar to the Feshbach resonance in ultracold gases driving up to about a maximum of about 0.2 the ratio between  $K_B T_c$  and the Fermi energy.

### III. ISOTOPE EFFECT

The isotope effect in  $H_3S$  [1] has provided a direct evidence of the involvement of the lattice degree of freedom in the pairing process. Therefore the isotope effect in sulfur hydrate at high pressure  $H_3S$  has been interpreted as ruling out theories of unconventional superconductivity (based only on spin liquid models or magnetic interactions) and supporting conventional theories of superconductivity based on the role of lattice fluctuations. However the standard BCS theory predicts a pressure independent isotope coefficient 0.5 while in non standard BCS theories, like in the multigap anisotropic BCS, the isotope coefficient deviates from 0.5 as in magnesium diboride where it is 0.26 [78]. From the new results reported by Droz et al. [2] we have extracted the isotope coefficient as a function of pressure shown in figure 3.

We can see in figure 3 large variations of the isotope coefficient reaching a minimum of 0.2 and first maximum reaching 0.5 at 170 GPa and a second peak at 240 GPa. The anomalous pressure dependent isotope coefficient has been found in cuprates superconductors as a function of doping [27, 69, 70] with anomalies where the chemical potential crosses Lifshitz transitions driven by pressure. Therefore the data in figure 3 indicate the possible presence of Lifshitz transitions in the pressure range showing near room temperature superconductivity.

Therefore in this work we have performed electronic structure calculations of the high pressure phase of sulfur hydrides  $H_3S$  with  $Im\bar{3}m$  lattice structure as function of pressure looking for Lifshitz transitions. Our band structure results show several bands crossings the chemical potential by increasing pressure, giving Lifshitz transitions and they have been correlated with a sharp peak in the density of states at the chemical potential. We calculate the large zero point motion of the hydrogen atoms inducing large energy fluctuations of the band edges spreading the effect of Lifshitz transitions over a large energy range.

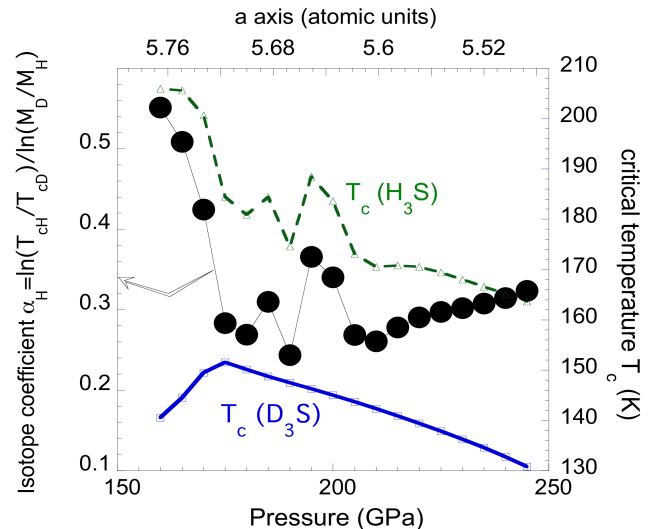


FIG. 3: (Color online) The pressure dependent isotope coefficient as a function of pressure (open red circles) calculated by interpolation of the experimental data of the critical temperature of  $H_3S$  (dashed green line) and  $D_3S$ ) solid red line reported by Droz et al. [2]

Our results support a large electron-phonon coupling and high frequencies of H-phonons contributing to rise of  $T_c$  [5, 10, 14] however we show the need of non standard BCS approach to describe the gaps in the appearing new Fermi surfaces at the multiple Lifshitz transitions controlled by pressure.

### IV. RESULTS.

We have performed band structure calculations of  $H_3S$  with  $Im\bar{3}m$  lattice symmetry made using the linear muffin-tin orbital (LMTO) method [79, 80] and the local spin-density approximation (LSDA) [81]. The details of the methods have been published earlier [82–85]. Self-consistent paramagnetic calculations are made for a unit cell containing 8 sites totally, and the basis set goes up through  $\ell=2$  for S and  $\ell=1$  for H. The Wigner-Seitz (WS) radii are  $0.38a$  for S and  $0.278a$  for H. The lattice constant  $a$  of the perovskite structure has been varied between 5.6 and 6.2 a.u.. The k-point mesh corresponds to 11 points between  $\Gamma$  and X, or 1331 points totally in  $1/8$  of the BZ. One band plot used a finer k-point mesh, 51 k-points between  $M$  and  $\Gamma$ .

The total DOS as a function of lattice parameter  $a$  are shown in Figs. 4-5 and the bands in Figs. 6-7. The charge within the H WS-sphere increases from 1.3 to 1.4 el./H when the lattice constant decreases from 6.2 to 5.6 a.u., and the H-s charge goes from 0.95 to 1.0. This fact justifies somewhat the use of LSDA for H even though atomic H with exactly 1 electron is best described by the

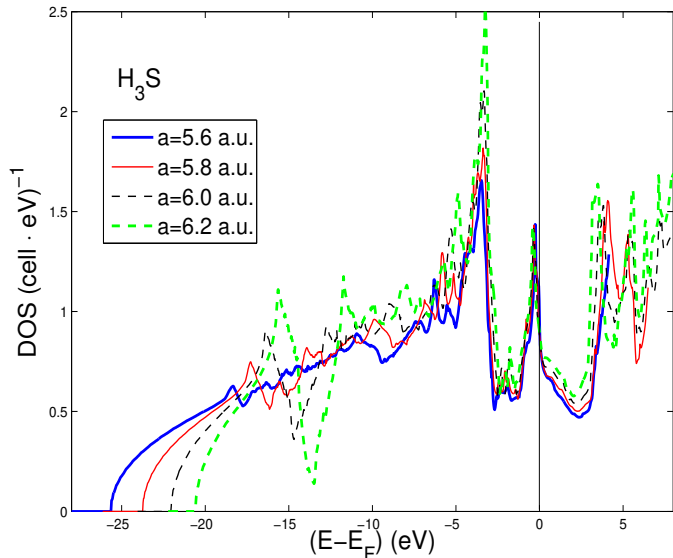


FIG. 4: (Color online) The total DOS for  $\text{H}_3\text{S}$  at 4 lattice constants.

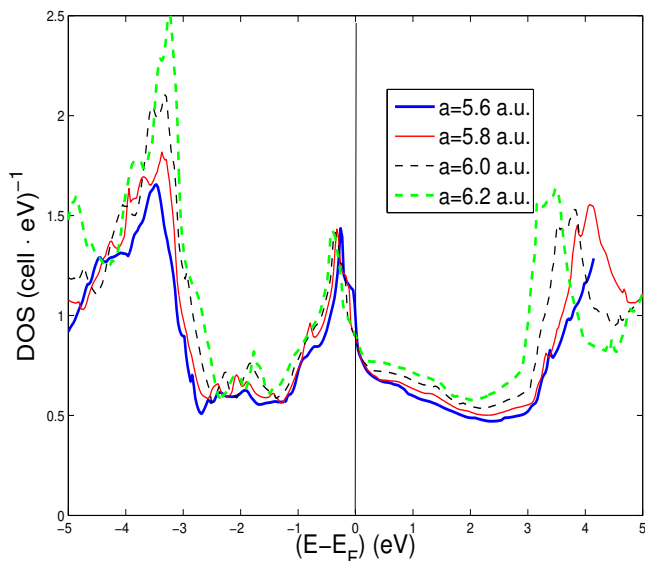


FIG. 5: (Color online) The DOS functions in Fig. 4 on a finer energy scale.

Hartree potential only. One spin-polarized calculation is made for the largest volume starting from an imposed ferro-magnetic (FM) configuration. All local FM moments converge to zero, which shows that FM and FM spin fluctuations are unlikely.

The S-2p core levels are always far below the valence band region at these pressures (about 12.2 Ry below  $E_F$ ). The pressure calculated as a surface integral using the virial theorem [86] is useful to get insight to the relative contribution from different atoms. These total pressures

( $P$ ) amount to 0.98 and -0.3 Mbar at the two extreme lattice constants. The partial S- and H-pressures increases much more on H than on S when the lattice constant is reduced. This together with the charge transfers, indicate that the S sublattice is more compressible than that of H. The charge transfer from S to H at high pressure will enforce the hardening of H.

TABLE I: Lattice constants  $a$ , DOS at  $E_F$  (in units of states/Ry/Cell), pressure  $P$ ,  $\lambda$ , and  $T_C$  estimated from the McMillan formula. The phonon moments for 600 and 1800 K for S and H, respectively, and  $\omega_{log}$  is 1500 K.

| $a$ (a.u.) | $N(E_F)$ | $P$ (GPa) | $\lambda$ | $T_C$ (K) |
|------------|----------|-----------|-----------|-----------|
| 5.6        | 13.5     | 215       | 1.0       | 143       |
| 5.8        | 12.3     | 150       | 0.81      | 109       |
| 6.0        | 12.0     | 95        | 0.73      | 93        |
| 6.2        | 12.2     | 50        | 0.70      | 73        |

More precise values of  $P$  are obtained from the calculated total energies, and we obtain 180 GPa for  $a=5.5$  a.u. and 73 GPa for  $a=6.1$  a.u., which agree well with ref. [10].

The lattice structure shows that the H sublattice forms chains along the principal axis directions. However, the general band structure appears to be 3-dimensional. The H-charge and the  $\ell$ -character at  $E_F$  is dominantly  $s$  (60-65 percent), and the hybridization between the  $s$ -electron and states on the S atoms away from the chains is large. The electron-phonon coupling constant  $\lambda$  is calculated in the Rigid Muffin-Tin Approximation (RMTA) [87, 88]. However, the matrix elements for  $d-f$ -scattering in S and  $p-d$  scattering in H are missing, which leads to some underestimation of the total  $\lambda$ . Our results are in agreement with the work of Papaconstantopoulos et al. [10] as shown in Table 1 where using the simple McMillan formula as in other papers [89] we obtain  $T_c$ 's of the order 145 and 75 K at the two lattice constants with total coupling strength going from 1.0 and 0.7. The different contributions to the total  $\lambda$  from each S and H atoms are comparable and  $\lambda$  itself is not unusually large. Using the McMillan formula valid only for a single effective band BCS system in the dirty limit, the high  $T_c$ .  $\omega_{log}$  is essentially given by the large phonon frequency pre-factor in the McMillan equation.

Our results shows the breakdown of the single band BCS approximation since we have detected several Lifshitz transitions controlled by the increasing pressure which drive at the chemical potential several bands where the Migdal approximation is not valid. From Figs. 7 it is seen that a band maximum (at " $\delta$ " in the figure) will cross  $E_F$  at about 2/3 of the  $\Gamma - M$  distance when  $a$  is  $\sim 5.8$  a.u., i.e. at large  $P$  when  $T_c$  is highest. The energy difference between  $E_F$  and this band maximum goes from -0.2 to +0.1 eV when  $a$  decreases from 6.2 to 5.6 a.u..

The top of the bands at  $\Gamma$  indicated by  $\alpha, \beta, \gamma$  and  $\delta$  are all above  $E_F$  at the highest  $P$ , but only the " $\alpha$ "-

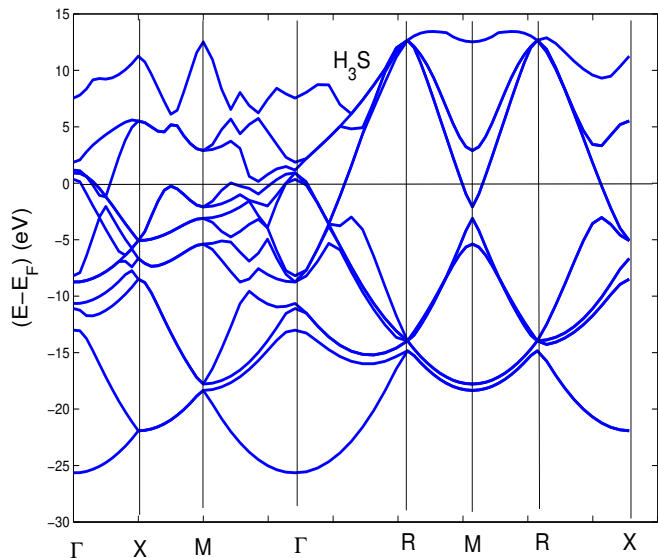


FIG. 6: (Color online) The band structure for  $\text{H}_3\text{S}$  at symmetry points plotted for  $a=5.6$  a.u..

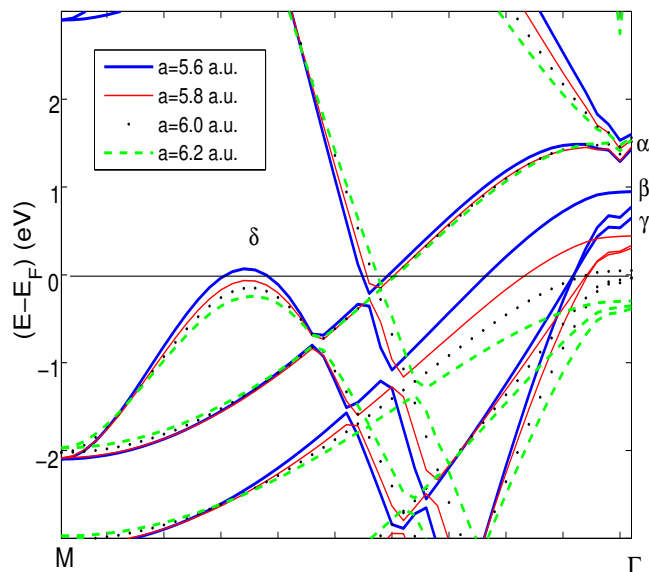


FIG. 7: (Color online) The band structure for  $\text{H}_3\text{S}$  between  $M$  and  $\Gamma$  for  $a=5.6$  a.u. to  $6.2$  a.u.. The LMTO band instability for s-bands for k-points near the  $\Gamma$ -point is the cause of the artifacts on the right-hand side of the figure.

band is insensitive to a change in volumes. The tops of the hole-like bands indicated by  $\beta$  and  $\gamma$  and  $\delta$  are below  $E_F$  at low  $P$ . The edges of these bands cross the chemical potential as function of  $P$  giving topological Lifshitz transitions with the appearing of new Fermi surface hole-pockets. The 100 meV fluctuations of the Fermi level in these bands drive the peak in the DOS slightly below ( $\sim 0.04$  eV)  $E_F$ , see Fig. 5 at  $E_F$ . Moreover since the

energy cut-off of the pairing interaction in this material is of the order of 100-200 meV all states in this energy range form pairs.

Our band structure has not yet taken into account the fact that thermal disorder and zero-point motion (ZPM) is large because of the small mass of H atoms. Such effects have been shown to be important in several different materials, even if their atomic masses are larger [90–92]. Lattice disorder can perturb spin waves and phonons in high- $T_c$  cuprates and might put a limit to very high  $T_c$ 's if superconductivity relies on very few phonons coupled with particular bands [93]. The Debye temperature for H phonons is high ( $\sim 1800\text{K}$ ) and thermal disorder beyond ZPM is not going to be large at  $T_c$ , but the disorder amplitude from ZPM is large already at low  $T$ . With a force constant  $K = M\omega^2$  of  $7 \text{ eV}/\text{\AA}^2$  we obtain an average amplitude  $u$  of the order  $0.15 \text{ \AA}$ . This is close to 10 percent of the H-H distance, which according to the Lindemann criterion suggests that the H sublattice is near melting. The  $u$ -amplitude for the S sublattice is normal, because of its large mass, and the S-lattice is probably important for the stability of the structure.

The zero point lattice fluctuation generates shifts of the Madelung potentials and therefore it modifies the band energies and leads to fluctuations of band edge ( $\Delta\epsilon$ ). The application of very high pressure makes the band structure very wide. As seen in Fig. 4, the band width is about 2 Ry for the high lying valence bands, and the S-s band overlaps with the S-p band. This makes the band dispersion and Fermi velocities high, and therefore the effects of energy band band is reduced if the chemical potential is far from band edges. The low- $T$  energy band fluctuations in materials with narrower band widths is known to be about 20 meV for  $u$  in the range  $0.03$ - $0.04 \text{ \AA}$ [90, 91, 93]. From an extrapolation of these values to the conditions in  $\text{H}_3\text{S}$  we estimate that the band energy fluctuation can be close to 100 meV for H-bands. Therefore when the chemical potential is tuned by pressure near a Lifshitz transition, so that the  $E_F$  in one of the bands is of the order of 100 meV the topology of the small Fermi surfaces made of small hole- or electron-pockets show strong dynamical fluctuations controlled by the zero point lattice fluctuations.

The consideration of ZPM motivates us to do calculations for supercells in which the lattice is disordered. Each atom is assigned randomized displacements,  $u_x, u_y, u_z$  is such a way that the distribution of all displacement amplitudes ( $|u|$ ) has a bell shaped (Gaussian) distribution with the FWHM width equal to the averaged displacement amplitude ( $u$ ) at the given  $T$ , as in ref. [90]. Here we consider a  $2\times 2\times 2$  extension of the normal unit cell with 64 atoms totally which permits to calculate  $u$  from 192 displacement vectors, which should be reasonably good statistics for calculation of  $u$ . However, because of the large mass difference between S and H we allow larger  $u$  for H ( $u_H$ ) than for S ( $u_S$ ). For small  $u$  it can be shown that correlation of vibrational movements and anharmonic terms are small [94]. This is a problem

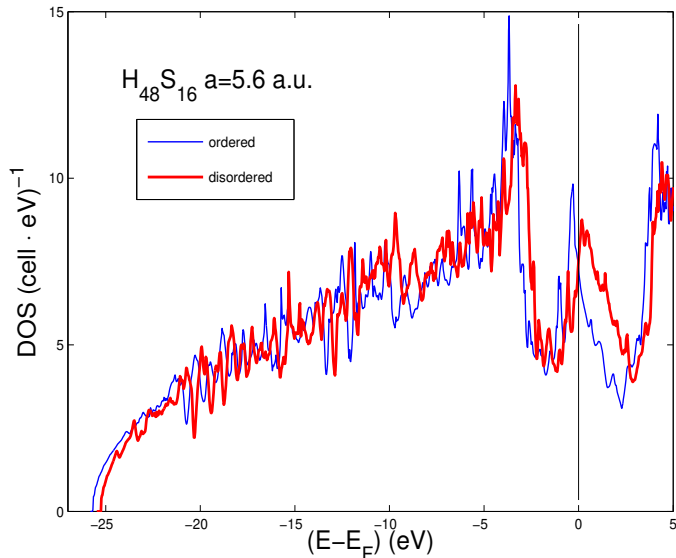


FIG. 8: (Color online) The DOS for  $\text{H}_3\text{S}$  for a cubic 64-site supercell. The (blue) thin line is the DOS for the perfectly ordered cell. The (red) heavy line shows the DOS for the disordered cell with  $u_S=0.01a$  and  $u_H=0.033a$ . The disorder for S corresponds to ZPM while the disorder for H is less than ZPM.

for vibrations of H since  $u_H$  is large, and in the generation of a disordered configuration for  $u_H/a=0.05$ , as for the expected ZPM, several pair of H come too close to each other. Therefore, we calculate the electronic structure for a supercell with  $u_S/a=0.01$  (which is close to the expected ZPM for S) and  $u_H/a=0.033$  (which is 2/3 of the expected ZPM for H).

The resulting DOS is shown in Fig. 8. The effect of ZPM is strong on the DOS peak just below  $E_F$ , which broadens and slips partially through  $E_F$ . This peak has a large fraction of H s- and p-states, while the peak further down (3-4 eV below  $E_F$ ) has less H-character and is less affected by disorder. The width at the base of the peak near  $E_F$  is about 2 eV in the ordered calculation. In the disordered case it has increased to about 3 eV. The broadening due to disorder is then 1 eV, even for  $u_H$  is smaller than the expected ZPM.

The superconducting gap ( $\Delta$ ) for  $T_c \approx 200\text{K}$  would be  $\sim 65$  meV at  $T=0$  according to the BCS-theory. With the parameters as in the calculation of  $\lambda$ , and  $\Delta = V$ , the amplitude for the potential modulation for phonons [95], one can estimate that  $u_\Delta$ , the displacement of phonons that lead to superconductivity should be  $\sim 0.02$  Å, i.e. less than the amplitude of ZPM for H, or comparable to the ZPM of S. Single phonon waves can be disturbed by thermal disorder [93], but since superconductivity seems to be resistant to perturbations from ZPM one may assume that either several phonon modes or the S sublattice are important for superconductivity. On the other hand, it is also seen that the effective DOS at  $E_F$  can increase

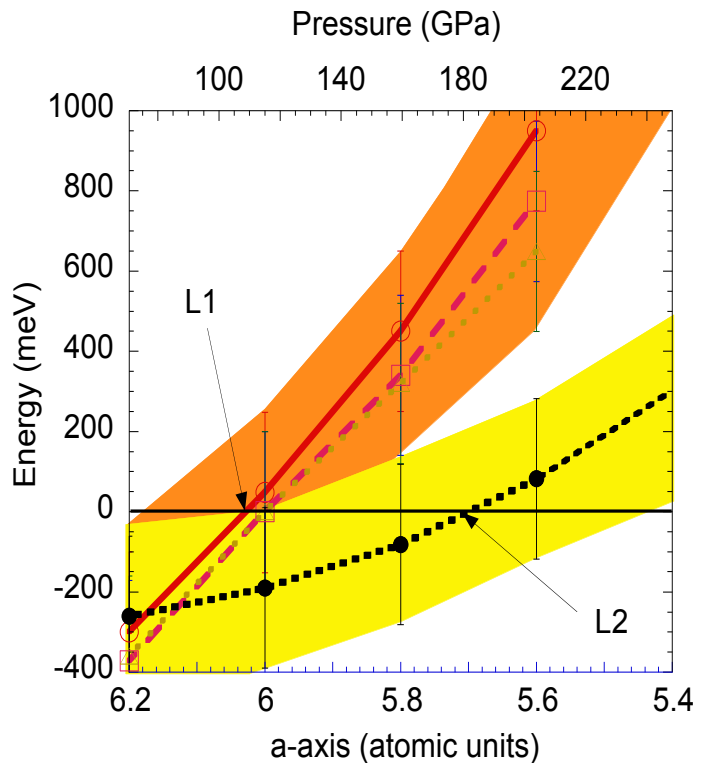


FIG. 9: (Color online) Energy shift of the tops of the  $\beta$ -hole-band (solid red line),  $\gamma$ -band (dashed red line) crossing the chemical potential at 100 GPa and the  $\delta$ -band (dotted black line) crossing the chemical potential at 180 GPa for  $\text{H}_3\text{S}$  between  $M$  and  $\Gamma$  points of the Brillouin zone

in the disordered structure, since  $E_F$  is close to a peak, which makes  $\lambda$  larger.

Figure 9 summarize our results showing the energy position of the top of the bands  $\beta$ ,  $\gamma_1$ ,  $\gamma_2$  and  $\delta$  as a function of pressure with the energy spread due to zero point lattice fluctuations indicated by the red ( $\beta$ ,  $\gamma_1$ ,  $\gamma_2$ ) and yellow area ( $\delta$ ). The shift of the energy position of the peak in the DOS near the chemical potential tracks exactly the top of the  $\delta$  band suggesting a Lifshitz transition of a quasi one-dimensional subband like in cuprates[25–27].

## V. CONCLUSION.

In this work we have shown that the electronic structure of sulfur hydrides  $\text{H}_3\text{S}$  with  $Im\bar{3}m$  lattice structure as function of pressure show Lifshitz transitions revealed by band crossings at  $E_F$  and a peak in the density of states near the Fermi level. Our results support the role of phonons [5, 10, 14?] but the presence of Lifshitz transitions tuned by pressure need the use of non standard BCS approach including the shape resonances with a key role of zero point lattice fluctuations. The emerging scenario is pairing in sulfur hydrides at high pressure in a dynamical landscape where key energy parameters have

all the same magnitude i.e, of the order of 100-200 meV: 1. the energy separation between the average position of the  $n^{\text{th}}$  band edge and the chemical potential, defined as the  $n^{\text{th}}$  Fermi energy controlling the "appearing or disappearing Fermi surface spot" Lifshitz transition in the Fermi surface topology, 2. the energy separation of a peak in the Density of States and the the band edge, usually controlling the "Neck opening" Lifshitz transition in the Fermi surface topology the amplitude of the energy cut are that predicted to favor the formation of the high temperature coherent state 3. the amplitude of the energy fluctuation of the critical Fermi surfaces associated with zero point lattice fluctuations 4. The energy of the pairing interaction defining the energy of the cut-off for the formations of pairs away from the chemical potential

In this scenario the BCS approximations used in the standard BCS theory are no more valid and the critical temperature is controlled not only by the energy of the changed boson,  $w_0$ , and the effective electron-phonon coupling (given by the product of the density of states times the electron-phonon coupling constant) but also by the condensation energy.

In fact in this situation the chemical shift from the normal to the condensed phase below  $T_c$  is no more negligible, and the coupling should be renormalized by a factor F, given by the quantum overlap of the condensed pairs [27, 45, 50, 67? ? -73]. The pressure dependence of this factor F can give shape resonances in the superconducting gaps appearing in superconductors made of multi-condensates near a Lifshitz transition Further work is needed to investigate i) the divergent amplitude of lattice fluctuations near the R3m to  $Im\bar{3}m$  2nd order structural transition around 180 GPa, ii) the large mass difference between H and S which requires the consideration of different amplitudes of  $u$  for the two types of atoms, and it should allow for  $E$  and  $k$  dependences for the energy fluctuations of Lifshitz transitions. The electronic band calculations should be extended to large supercells needed for more precise estimates of energy fluctuations of the electronic structure associated with spacial structural fluctuations. With think that the discovery of superconductivity in sulfur hydrates very near room temperature has narrowed the number of possible road maps toward new functional superconducting materials. Further fundamental research on the mechanism of room temperature superconductivity in these new phase of matter are needed to clarify this emerging physical scenario and they will allow the definition of a protocol for the material design of new functional room temperature superconductors.

## APPENDIX

The standard BCS theory in undergraduate courses considers a homogeneous single band metal and describes the cooper pairing in weak coupling limit as due to quantum exchange of a low energy phonon between two high

energy electrons at the Fermi level in the Migdal approximation where the gap energy is much smaller than the Fermi energy and the gap to critical temperature ratio is equal to 1.75. Non standard BCS theories diverge substantially from the standard BCS theory. Let us simplify a long story by classify 7 different non standard BCS theories. Let us start with the first group considering a single effective band, in a dirty limit, giving a single condensate:

1A) the standard strong coupling Eliashberg theories considering a high energy phonon or vibron (a quantum of intramolecular vibration) interacting with electrons having a large Fermi energy  $\omega_0/E_F \ll 1$ . Most of previous theories for high  $T_c$  in sulfur hydrates have proposed this approach for a large phonon frequency and strong coupling;

1B) the theories considering the case of a low density electron gas beyond the Migdal approximation  $\omega_0/E_{Fn} > 1$  where the single condensate is formed by BEC condensation or by BEC-BCS crossover  $\Delta_n/E_F \sim 1$ ,

1C) non standard BCS theories which consider pairing mediated by electronic excitations, called exciton theories.

The second group of non standard BCS theories considers the anisotropic BCS theory, in the clean limit, therefore they focus on multi-gap superconductivity where multiple gaps are formed in different spots of the k-space. These non standard BCS theories consider metals with multiple bands with different symmetry crossing the chemical potential:

2A) The multiband BCS model where all multiple Fermi surfaces in the BCS limit coexist;

2B) the Fermi-Bose model where the Fermi level of a first band is degenerate with a single level, occupied by paired electrons. Here a BCS condensate coexist with bosons which undergoes a Bose condensation;

2C) the extreme case of superconductivity driven mostly by exchange like interband pairing with very weak, or no intraband pairing;

2D) The theory of *shaperesonance* in superconducting gaps for multi-condensates with a small interband pairing, emerging in metals where: a first small charge density in small Fermi surfaces form condensates in the BEC-BCS crossover, beyond Migdal approximation, which coexists with a second large density of charges in large Fermi surfaces form BCS condensates.

A third group of theories consider the case of systems with relevant electronic and lattice inhomogeneity with insulator to superconductor transitions in presence of nanoscale phase separation where the Josephson-like interaction between localized condensates play a key role.

Here we focus on the *shaperesonance* (2D) mechanism, already proposed for cuprates, [25–27, 67–70] diborides [46, 50] and iron based superconductors [71–73]. This mechanism (2D) is proposed here for sulfur hydrides at very high pressure following the reported evidence for Lifshitz transitions driven by high pressure. We recall below the non standard BCS theory for shape resonances.

Let us consider a system made of multiple bands with index  $n$ , having a steep free electron like dispersion in the  $x$  direction and a flat band-like dispersion in the  $y$  direction. The energy separation between the chemical potential and the bottom of the  $n$ -th band defines the Fermi energy of the  $n$ -th band. This formulation of the BCS was proposed for complex systems in presence of one-dimensional lattice modulation or one-dimensional charge density waves which coexist with the superconducting condensate like in magnesium diborides, A15, cuprates and we propose here should be applied to sulfur hydrate at high pressure.

The formula for the superconducting critical temperature  $T_c$  in a anisotropic multigap non standard BCS scheme is given by the linearized BCS equation considering the simplest case of a two dimensional system [27] but the extension to three dimensional system [50] is trivial.

$$\Delta_{n,k_y} = -\frac{1}{2N} \sum_{n',\mathbf{k}'} V_{\mathbf{k},\mathbf{k}'}^{n,n'} \frac{\tanh\left(\frac{E_{n,k_y} + \epsilon_{k_x} - \mu}{2T_c}\right)}{E_{n,k_y} + \epsilon_{k_x} - \mu} \Delta_{n',k'_y}, \quad (1)$$

where the energy dispersion is measured with respect to the chemical potential.

The multiple gaps  $\Delta_{n,k_y}$  in multiple bands  $n$  with flat band-like dispersion in the  $y$  direction and steep free-electron-like dispersion in the  $x$  direction are related by a self consistent equation at ( $T = 0$ ) in the multigap anisotropic BCS theory which for a simple model of a two dimensional metal with a one-dimensional superlattice modulation in the  $y$ -direction is given by

$$\Delta_{n,k_y} = -\frac{1}{2N} \sum_{n',k'_y,k'_x} \frac{V_{\mathbf{k},\mathbf{k}'}^{n,n'} \Delta_{n',k'_y}}{\sqrt{(E_{n',k'_y} + \epsilon_{k'_x} - \mu)^2 + \Delta_{n',k'_y}^2}}, \quad (2)$$

where  $N$  is the total number of wave-vectors in the discrete summation,  $\mu$  is the chemical potential,  $V_{\mathbf{k},\mathbf{k}'}^{n,n'}$  is the effective pairing interaction

$$\begin{aligned} V_{\mathbf{k},\mathbf{k}'}^{n,n'} &= \tilde{V}_{\mathbf{k},\mathbf{k}'}^{n,n'} \\ &\times \theta(\omega_0 - |E_{n,k_y} + \epsilon_{k_x} - \mu|) \theta(\omega_0 - |E_{n',k'_y} + \epsilon_{k'_x} - \mu|) \end{aligned} \quad (3)$$

Here we take account of the interference effects between the wave functions of the pairing electrons in the different bands, where  $n$  and  $n'$  are the band indexes,  $k_y$  ( $k'_y$ ) is the superlattice wave-vector and  $k_x$  ( $k'_x$ ) is the component of the wave-vector in the free-electron-like direction of the initial (final) state in the pairing process.

$$\begin{aligned} \tilde{V}_{\mathbf{k},\mathbf{k}'}^{n,n'} &= -\frac{\lambda_{n,n'}}{N_0} S \\ &\times \int_S \psi_{n',-k'_y}(y) \psi_{n,-k_y}(y) \psi_{n,k_y}(y) \psi_{n',k'_y}(y) dx dy, \end{aligned} \quad (4)$$

where  $N_0$  is the DOS at  $E_F$  without the lattice modulation,  $\lambda_{n,n'}$  is the dimensionless coupling parameter,  $S = L_x L_y$  is the surface of the plane and  $\psi_{n,k_y}(y)$  are the eigenfunctions in the 1D superlattice. The gap equation need to be solved iteratively. The anisotropic gaps dependent on the band index and on the superlattice wave-vector  $k_y$ . According with Leggett [55] the ground-state BCS wave function corresponds to an ensemble of overlapping Cooper pairs at weak coupling (BCS regime) and evolves to molecular (non-overlapping) pairs with bosonic character and this approach remains valid also if a particular band is in the BC-BCS crossover and beyond Migdal approximation because all other many bands are in the BCS and Migdal approximation.

However to be correct in this anomalous regime the BCS equation for the gap should be coupled to the equation that fixes the fermion density: with increasing coupling (or decreasing density), the chemical potential  $\mu$  results strongly renormalized with respect to the Fermi energy  $E_F$  of the non interacting system, and approaches minus half of the molecular binding energy of the corresponding two-body problem in the vacuum.

In the case of a Lifshitz transition, described in this paper, all electrons in the new appearing Fermi surface condense forming a condensate in the BEC-BCS crossover. Therefore it is essential that the chemical potential in the superconducting phase should be renormalized by the gap opening at any chosen value of the charge density  $\rho$ :

$$\begin{aligned} \rho &= \frac{1}{L_x L_y} \sum_n \sum_{k_x, k_y}^{N_b} \left[ 1 - \frac{E_{n,k_y} + \epsilon_{k_x} - \mu}{\sqrt{(E_{n,k_y} + \epsilon_{k_x} - \mu)^2 + \Delta_{n,k_y}^2}} \right] \\ &= \frac{\delta k_y}{\pi} \sum_{n=1}^{N_b} \sum_{k_y=0}^{\pi/l_p} \int_0^{\epsilon_{min}} d\epsilon \frac{2N(\epsilon)}{L_x} + \int_{\epsilon_{min}}^{\epsilon_{max}} d\epsilon \frac{N(\epsilon)}{L_x} \\ &\times \left( 1 - \frac{E_{n,k_y} + \epsilon_{k_x} - \mu}{\sqrt{(E_{n,k_y} + \epsilon_{k_x} - \mu)^2 + \Delta_{n,k_y}^2}} \right), \end{aligned} \quad (5)$$

where

$$\begin{aligned} \epsilon_{min} &= \max [0, \mu - \omega_0 - E_{n,k_y}], \\ \epsilon_{max} &= \max [0, \mu + \omega_0 - E_{n,k_y}], \\ N(\epsilon) &= \frac{L_x}{2\pi \sqrt{\frac{\epsilon}{2m}}}, \end{aligned}$$

and  $N_b$  is the number of the occupied bands,  $L_x$  and  $L_y$  are the size of the considered surface and the increment in  $k_y$  is taken as  $\delta k_y = 2\pi/L_y$ .

- 
- [1] A.P. Drozdov, M.I. Eremets, I.A. Troyan, preprint arXiv:1412.0460, (1 December 2014) URL <http://arxiv.org/abs/1412.0460>.
- [2] A.P. Drozdov, M.I. Eremets, I.A. Troyan, V. Ksenofontov, S.I. Shylin, preprint arXiv:1506.08190 (30 June 2015) URL <http://arxiv.org/abs/1506.08190>.
- [3] M.I. Eremets in "Superstripes 2015" A. Bianconi (ed.) Science Series Vol. 6, p.286 (Superstripes Press, Rome, 2015) ISBN:9788866830382.
- [4] E. Cartlidge, Nature (29 June 2015), ISSN 1476-4687, doi:10.1038/nature.2015.17870
- [5] D. Duan, Y. Liu, F. Tian, et al. *et al*, Sci. Rep. **4**, 6968 (2014).
- [6] A. O. Lyakhov, A. R. Oganov, H.T. Stokes, Q. Zhu, Comput. Phys. Commun. **184**, 1172 (2013).
- [7] D. Duan, X. Huang, F. Tian, D. Li, H. Yu, Y. Liu, Y. Ma, B. Liu, and T. Cui, Phys. Rev. B **91**, 180502 (2015).
- [8] Jos A. Flores-Livas, Antonio Sanna, E.K.U. Gross High temperature superconductivity in sulfur and selenium hydrides at high pressure preprint arXiv:1501.06336v1 (26 Jan 2015)
- [9] Shoutao Zhang, Yanchao Wang, Jurong Zhang, Hanyu Liu, Xin Zhong, Hai-Feng Song, Guochun Yang, Lijun Zhang, Yanming Ma preprint arXiv:1502.02607 (9 Feb. 2015)
- [10] D. Papaconstantopoulos, B.M. Klein, M.J. Mehl, W.E. Pickett, Phys. Rev. B **91**, 184511 (2015).
- [11] I. Errea, M. Calandra, C. J. Pickard, J. Nelson, R. J. Needs, Y. Li, H. Liu, Y. Zhang, Y. Ma, F. Mauri Phys. Rev. Lett. **114**, 157004 (2015).
- [12] N. Bernstein, C.S. Hellberg, M.D. Johannes, I.I. Mazin, M.J. Mehl, Phys. Rev. B **91**, 060511 (2015).
- [13] A. P. Durajski, R. Szczesniak, Y. Li Physica C: Superconductivity and its Applications **515**, 1-6(2015)
- [14] R. Akashi, M. Kawamura, S. Tsuneyuki, Y. Nomura, and R. Arita, Preprint arXiv:1502.00936 (Feb 2015).
- [15] J. E. Hirsch, F. Marsiglio Physica C: Superconductivity and its Applications **511**, 45-49 (2015) .
- [16] N. W. Ashcroft, Physical Review Letters **21**, 1748 (1968)
- [17] V. L. Ginzburg and D. A. Kirzhnits, "High temperature superconductivity" Consultants Bureau, Plenum Press, (New York, 1982).
- [18] C. F. Richardson and N. W. Ashcroft Phys. Rev. Lett. **78**, 118 (1997)
- [19] E. G. Maksimov and Savrasov, Solid State Communications **119**, 569 (2001)
- [20] N. W. Ashcroft, Physical Review Letters **92**, 187002 (2004)
- [21] N. W. Ashcroft, In Bianconi, A. (ed.) Symmetry and Heterogeneity in High Temperature Superconductors, vol. 214 of NATO Science Series II: Mathematics, Physics and Chemistry, **3-20** (Springer Netherlands, 2006).
- [22] E. Babaev, A. Sudbo, N. W. Ashcroft Nature **431**, 666-668 (2004)
- [23] E. G. Maksimov and O. V. Dolgov, Physics-Uspokhi **40**, 933 (2007).
- [24] Kazutaka Abe, N. W. Ashcroft Phys. Rev. B, **88**, 174110 (2013).
- [25] A. Bianconi, Solid State Communications **89**, 933 (1994).
- [26] A. Perali, A. Bianconi, A. Lanzara and N.L. Saini Solid State Commun. **100**, 181 (1996)
- [27] A. Bianconi, A. Valletta, A. Perali, N.L. Saini, Physica C: Superconductivity **296**, 269 (1998).
- [28] G. Bianconi Superconductor-insulator transition on annealed complex networks Physical Review E **85**, 061113 (2012).
- [29] A. Bianconi, S. Agrestini, G. Bianconi, D. Di Castro, N.L. Saini Journal of alloys and compounds **317**, 537-541 (2001)
- [30] Xin Zhong, Hui Wang, Jurong Zhang, Hanyu Liu, Shoutao Zhang, Hai-Feng Song, Guochun Yang, Lijun Zhang, Yanming Ma preprint arXiv:1503.00396 (march 2015)
- [31] Changbo Chen, Fubo Tian, Defang Duan, et al. The Journal of Chemical Physics, **140**, 114703 (2014).
- [32] Pugeng Hou, Xiusong Zhao, Fubo Tian, et al. RSC Adv., **5**, 5096-5101 (2015). doi:10.1039/c4ra14990d
- [33] L. Paulatto, I. Errea, M. Calandra, F. Mauri Phys. Rev. B, **91**, 054304 (2014).
- [34] Yanhui Liu, Fubo Tian, Xilian Jin, et al. Solid State Communications, **147**, 1126-129 (2008).
- [35] G. R. Stewart, Physica C: Superconductivity and its Applications **514**, 28 (2015).
- [36] J. Friedel, Phase transitions, electron-phonon couplings in perfect crystals modulated structures in "Electron-Phonon Interactions and Phase Transitions" Springer Science & Business Media, NATO Advanced Study Institute (1977).
- [37] W. L. McMillan, Superconductivity, and martensitic transformations in A-15 compounds in "Electron-Phonon Interactions and Phase Transitions" Springer Science & Business Media, NATO Advanced Study Institute (1977).
- [38] L. R. Testardi, Structural phase transitions, superconductivity in A15 compounds in "Electron-Phonon Interactions and Phase Transitions" Springer Science & Business Media, NATO Advanced Study Institute (1977).
- [39] L. R. Testardi, Structural instability and superconductivity in A-15 compounds. Reviews of Modern Physics **47**, 637 (1975)
- [40] M. Takeda, H. Yoshida, H. Endoh, and H. Hashimoto, Journal of Microscopy **151**, 147-157 (1988).
- [41] M. Arita, H. U. Nissen, Y. Kitano, and W. Schauer, Journal of Solid State Chemistry **107**, 76 (1993)
- [42] N. L. Saini, M. Filippi, Z. Wu, H. Oyanagi, H. Ihara, A. Iyo, S. Agrestini, and A. Bianconi, Journal of Physics: Condensed Matter **14**, 13543 (2002)
- [43] H. Suhl, B. T. Matthias, and L. R. Walker, Physical Review Letters **3**, 552 (1959).
- [44] G. A. Ummarino, R. S. Gonnelli, S. Massidda, and A. Bianconi, Physica C: Superconductivity **407**, 121 (2004).
- [45] H. J. Choi, M. L. Cohen, and S. G. Louie, Physical Review B **73**, 104520 (2006).
- [46] A. Bianconi, D. Di Castro, S. Agrestini, G. Campi, N. L. Saini, A. Saccone, S. De Negri, M. Giovannini, Journal of Physics: Condensed Matter **13**, 7383 (2001).
- [47] T. Yildirim, O. Glseren, J. W. Lynn, C. M. Brown, T. J. Udovic, Q. Huang, N. Rogado, K. A. Regan, M. A. Hayward, J. S. Slusky, et al., Physical Review Letters **87** 037001 (2001).
- [48] G. Campi, E. Cappelluti, T. Proffen, X. Qiu, E. S. Bozin, Billinge, S. Agrestini, N. L. Saini, and A. Bianconi, The

- European Physical Journal B - Condensed Matter and Complex Systems, **52**, 15 (2006).
- [49] L. Simonelli, V. Palmisano, M. Fratini, M. Filippi, P. Parisiades, D. Lampakis, E. Liarokapis, and A. Bianconi, Phys. Rev. B **80**, 014520 (2009).
- [50] D. Innocenti, N. Poccia, A. Ricci, A. Valletta, S. Caprara, A. Perali, A. Bianconi, Phys. Rev. B **82**, 184528 (2010).
- [51] Q. Chen, J. Stajic, S. Tan, and K. Levin, Physics Reports **412**, 1 (2005),
- [52] L. Boeri, E. Cappelluti, and L. Pietronero, Physical Review B **71**, (2005).
- [53] A. Perali, P. Pieri, and G.C. Strinati Phys. Rev. Lett. **93**, 100404 (2004).
- [54] J. Bardeen, L.N. Cooper, J.R. Schrieffer Phys. Rev. **108**, 1175 (1957)
- [55] A. J. Leggett, in Modern Trends in the Theory of Condensed Matter, edited by by A. Pekalski and R. Przystawa, Lecture Notes in Physics Vol. **115** (Springer-Verlag, Berlin, 1980), p. 13.
- [56] N.N. Bogolyubov. V.V. Tolmachev, D. V. Shirkov Fortschr. Physik **6**, 605 (1958)
- [57] L. P. Gor'kov, J. Exptl. Theoret. Phys. U.S.S.R. **34**, 735 (1958) ; translation in English Soviet Physics JEPT **7**, 505 (1958)
- [58] B.D. Josephson Physics Letters **1**, 251 (1962)
- [59] J. M. Blatt Theory of Superconductivity, Academic Press, New York (1964)
- [60] James F. Annett Superconductivity, Superfluids and Condensates Oxford University Press, Oxford, 2004
- [61] B. V. Svistunov, E.S. Babaev, N. V. Prokof'ev Superfluid States of Matter CRC Press, 2015 -
- [62] I. M. Lifshitz, Sov. Phys. JETP **11**, 1130 (1960).
- [63] A. Varlamov, V. Egorov, A. Pantsulaya, Advances in Physics **38**, 469 (1989).
- [64] K. Kugel, A. Rakhmanov, A. Sboychakov, N. Poccia, and A. Bianconi, Physical Review B **78**, 165124 (2008).
- [65] A. Bianconi, N. Poccia, A. O. Sboychakov, A. L. Rakhmanov, and K. I. Kugel, Supercond. Sci. Technol. **28**, 024005 (2015).
- [66] A. Guidini and A. Perali, Supercond. Sci. Technol. **27**, 124002 (2014).
- [67] A. Bianconi, Journal of Superconductivity **18**, 625 (2005).
- [68] A. Bianconi, Iranian Journal of Physics Research **6**, 139 (2006).
- [69] A. Perali, D. Innocenti, A. Valletta, and A. Bianconi, Superconductor Science and Technology **25**, 124002 (2012).
- [70] D. Innocenti and A. Bianconi, J Supercond Nov Magn **26**, 1319 (2013).
- [71] R. Caivano, et al. Superconductor Science and Technology **22**, 014004 (2009).
- [72] D. Innocenti, A. Valletta, A. Bianconi, Journal of Superconductivity and Novel Magnetism **24**, 1137 (2011).
- [73] A. Bianconi, Nature Physics **9**, 536 (2013). URL <http://dx.doi.org/10.1038/nphys2738>.
- [74] A. A. Kordyuk, et al. Journal of Superconductivity and Novel Magnetism **26**, 2837 (2013)
- [75] A. A. Kordyuk, Low Temperature Physics **41**, 319-341 (2015).
- [76] C. Liu, et al., Physical Review B **84**, 020509 (2011)
- [77] S. Ideta, et al., Physical Review Letters **119**, 107007+ (2013)
- [78] S. L. Bud'ko, G. Lapertot, C. Petrovic, C. E. Cunningham, N. Anderson, P. C. Canfield Phys. Rev. Lett., **86**, 1877 (2001).
- [79] O.K. Andersen, Phys. Rev. B **12**, 3060 (1975).
- [80] B. Barbiellini, S.B. Dugdale and T. Jarlborg, Comput. Mater. Sci. **28**, 287 (2003).
- [81] W. Kohn and L.J. Sham, Phys. Rev. **140**, A1133 (1965); O. Gunnarsson and B.I. Lundquist, Phys. Rev. B **13**, 4274 (1976).
- [82] T. Jarlborg, A.A. Manuel and M. Peter, Phys. Rev. B **27**, 4210, (1983).
- [83] T. Jarlborg, E.G. Moroni and G. Grimvall, Phys. Rev. B **55**, 1288, (1997).
- [84] E.G. Moroni, G. Grimvall and T. Jarlborg, Phys. Rev. Lett. **76**, 2758, (1996).
- [85] T. Jarlborg and A. Bianconi, Phys. Rev. B **87**, 054514, (2013).
- [86] D. Pettifor, J. Phys. F: Metal Phys. **7**, 1009, (1977).
- [87] G.D. Gaspari and B.L. Gyorffy, Phys. Rev. Lett. **28**, 801, (1972).
- [88] M. Dacorogna, T. Jarlborg, A. Junod, M. Pelizzone and M. Peter, J. Low Temp. Phys. **57**, 629, (1984).
- [89] W.L. McMillan, Phys. Rev. **167**, 331, (1968).
- [90] T. Jarlborg, Phys. Rev. B **59**, 15002, (1999).
- [91] T. Jarlborg, P. Chudzinski and T. Giamarchi, Phys. Rev. B **85**, 235108, (2012).
- [92] T. Jarlborg, Phys. Rev. B **89**, 184426 (2014).
- [93] T. Jarlborg, J. of Supercond. and Novel Magn., **28**, 1231, (2014) DOI: 10.1007/s 10948-014-2897-1
- [94] G. Grimvall, *Thermophysical properties of materials*. (North-Holland, Amsterdam, 1986).
- [95] T. Jarlborg, Solid State Commun. **151**, 639, (2011).